


Role of [¹⁸F]FDG PET/CT in the differential diagnosis of a supraclavicular lump: neurofibromatosis disease

Ana Moreno-Ballesteros¹ , Maria De Bonilla-Candau², Javier Mohigefer³, Marta Moreno-Ballesteros⁴, Francisco Javier Garcia-Gomez¹

¹Servicio de Medicina Nuclear, Hospital Universitario Virgen Macarena, Sevilla, Spain

²Servicio de Medicina Nuclear, Hospital Universitario Puerta del Mar, Cadiz, Spain

³Servicio de Anatomia Patologica, Hospital Universitario Virgen Macarena, Sevilla, Spain

⁴Servicio de Cirugía General, Hospital de Merida, Badajoz, Spain

[Received: 6 VI 2022; Accepted: 4 IX 2022]

Abstract

We report a 31-year-old male with a history of left forearm neuroma surgically removed, consulting for a supraclavicular bultoma congruent with the supradiaphragmatic lymphoproliferative syndrome in computed tomography (CT) scan. [¹⁸F]FDG PET/CT images helped to establish the most diagnostic yield lesion for the biopsy, and allowed an accurate staging of the neurofibromatosis (NF) disease, leading to the most appropriate therapeutic option for the patient.

KEY words: [¹⁸F]FDG; NF; PET/CT; neurofibroma; differential diagnosis; bultoma

Nucl Med Rev

We present a 31-year-old male with a history of left forearm neuroma surgically removed in 2016. At this time, he consulted for a supraclavicular bultoma with computed tomography (CT) findings of supradiaphragmatic lymphatic involvement (right jugulocarotid, left supraclavicular, deltoid, and bilateral mediastinal regions) morphologically congruent with a lymphoproliferative syndrome. Therefore, a staging [¹⁸F]FDG PET/CT was requested.

The skull-base-to-mid-thigh imaging (Fig. 1) evidenced some metabolically positive lymphadenopathies in both supraclavicular regions reaching a size of 6.4 cm (SUVmax 10.04) in the left (white arrow), with no pathological [¹⁸F]FDG deposits in right jugulocarotid region and mediastinum. In infradiaphragmatic territories, multiple subcentimetric lymphadenopathies were observed (SUVmax 3.4) highlighting a larger paraaortic node (4.4 cm; SUVmax 9.63; black arrow). In addition, two hypermetabolic rounded lesions contiguous to the left deltoids muscle (1.7 cm and SUVmax of 4.87; blue arrow) and right anterior rectus muscle (2.3 cm; SUVmax 3.81; green arrow) were visualized. In light of these findings, it was mandatory to discard malignancy.

Based on above mentioned metabolic activity, the left supraclavicular lymphadenopathy was biopsied (Fig. 2) revealing in the hematoxylin-eosin stain low-grade spindle cell proliferation (black arrow) within a myxoid stroma (blue circle), emphasizing thick eosinophilic collagen fibers also known as “shredded carrots” (red arrows). These results were congruent with neurofibroma. Added to the previous antecedent of the neuroma, the patient was diagnosed with neurofibromatosis (NF) and staged as a diffuse disease by PET/CT, thus surgical alternative was dismissed and systemic treatment with Selumetinib was proposed.

Neurofibromas are the most prevalent benign peripheral nerve sheath tumor classically associated with neurofibromatosis (NF) but also can appear as solitary lesions [1, 2]. Those related to NF carry an increased risk of malignant transformation (2–13%), consequently, some cut-off values of SUVmax have been proposed based on a SUVmax greater than 3.2 [3] and lesion-to-liver (T/L) values over 1.5 [4, 5, 6] but the role of [¹⁸F]FDG PET/CT remains still under discussion at this point [7, 8]. Complete surgical excision is the treatment of choice in most patients, retaining systemic treatments such as recently FDA-approved selumetinib (tyrosine kinase inhibitor) for diffuse NF cases [9]. In this case, the completion of [¹⁸F]FDG PET/CT helped to establish the most diagnostic yield lesion for the biopsy, and allowed an accurate staging of the NF disease, leading to the most appropriate therapeutic option.

Correspondence to: Ana Moreno-Ballesteros
 Servicio de Medicina Nuclear. Hospital Universitario Virgen Macarena,
 Avenida Dr Fedriani nº3, 41009 Sevilla, Spain,
 phone: +34 662 69 87 66, e-mail: anamoreno_ballesteros@hotmail.com

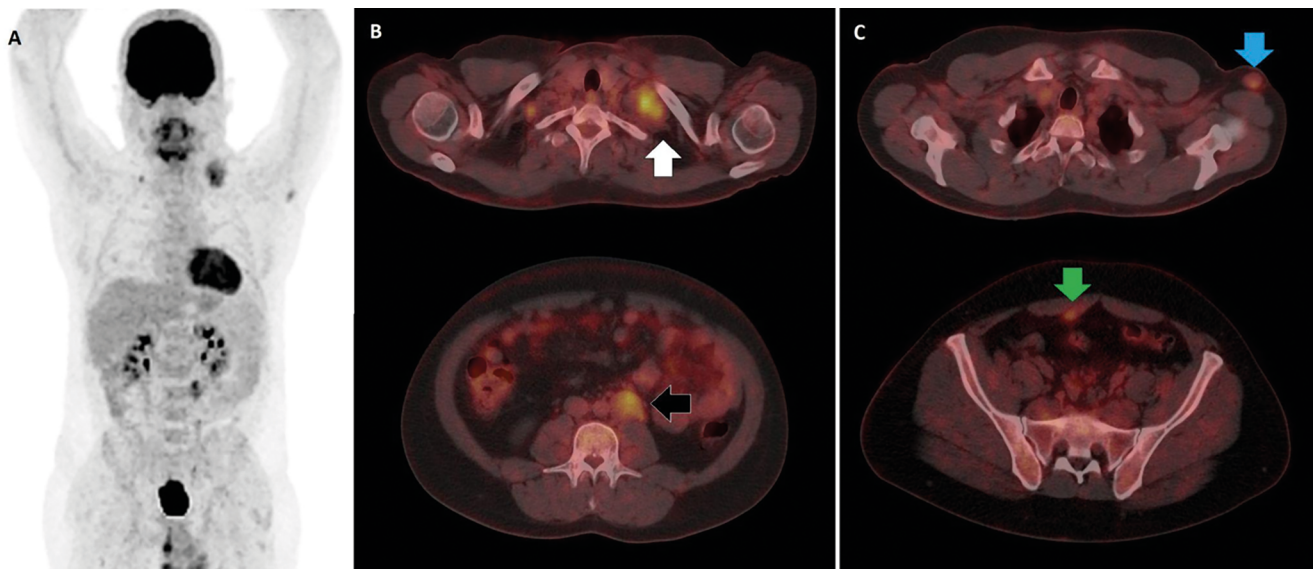


Figure 1. [^{18}F]FDG MIP (A) and fused images of most [^{18}F]FDG avid lymphadenopathy (B) in left supraclavicular (white arrow) and left paraaortic territories (black arrow). Rounded pathological soft tissue lesions (C) adjacent to deltoids (blue arrow) and right rectus anterior muscles (green arrow)

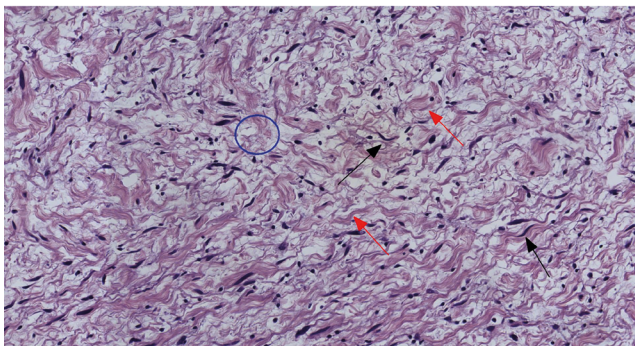


Figure 2. Microscope image of supraclavicular lymphadenopathy biopsy with HE stain $\times 20$ demonstrating myxoid stroma (blue circle) with low-grade spindle cell proliferation (black arrow) and thick eosinophilic collagen fibers also known as “shredded carrots” (red arrows) congruent with neurofibroma

References

1. Ferner R, O Doherty M. Neurofibroma and schwannoma. *Curr Opin Neurol.* 2002; 15(6): 679–684, doi: [10.1097/01.wco.0000044763.39452.aa](https://doi.org/10.1097/01.wco.0000044763.39452.aa).
2. Strike SA, Puhaindran ME. Nerve tumors of the upper extremity. *Clin Plast Surg.* 2019; 46(3): 347–350, doi: [10.1016/j.cps.2019.02.008](https://doi.org/10.1016/j.cps.2019.02.008), indexed in Pubmed: [31103079](https://pubmed.ncbi.nlm.nih.gov/31103079/).
3. Obuchowski NA. Receiver operating characteristic curves and their use in radiology. *Radiology.* 2003; 229(1): 3–8, doi: [10.1148/radiol.2291010898](https://doi.org/10.1148/radiol.2291010898), indexed in Pubmed: [14519861](https://pubmed.ncbi.nlm.nih.gov/14519861/).
4. Mantaka P, Strauss AD, Moehler M, et al. Detection of treated liver metastases using fluorine-18-fluorodeoxyglucose (FDG) and positron emission tomography (PET). *Anticancer Res.* 1999; 19: 4443–4450, indexed in Pubmed: [10650790](https://pubmed.ncbi.nlm.nih.gov/10650790/).
5. Chirindel A, Chaudhry M, Blakeley JO, et al. 18F-FDG PET/CT qualitative and quantitative evaluation in neurofibromatosis type 1 patients for detection of malignant transformation: comparison of early to delayed imaging with and without liver activity normalization. *J Nucl Med.* 2015; 56(3): 379–385, doi: [10.2967/jnumed.114.142372](https://doi.org/10.2967/jnumed.114.142372), indexed in Pubmed: [25655626](https://pubmed.ncbi.nlm.nih.gov/25655626/).
6. Van Der Gucht A, Zehou O, Djelani-Ahmed S, et al. Metabolic tumour burden measured by 18F-FDG PET/CT predicts malignant transformation in patients with neurofibromatosis type-1. *PLoS One.* 2016; 11(3): e0151809, doi: [10.1371/journal.pone.0151809](https://doi.org/10.1371/journal.pone.0151809), indexed in Pubmed: [26987124](https://pubmed.ncbi.nlm.nih.gov/26987124/).
7. Ahlawat S, Blakeley J, Montgomery E, et al. Schwannoma in neurofibromatosis type 1: a pitfall for detecting malignancy by metabolic imaging. *Skeletal Radiol.* 2013; 42(9): 1317–1322, doi: [10.1007/s00256-013-1626-3](https://doi.org/10.1007/s00256-013-1626-3), indexed in Pubmed: [23649401](https://pubmed.ncbi.nlm.nih.gov/23649401/).
8. Brinkman M, Jentjens S, Boone K, et al. Evaluation of the most commonly used (semi-)quantitative parameters of 18F-FDG PET/CT to detect malignant transformation of neurofibromas in neurofibromatosis type 1. *Nucl Med Commun.* 2018; 39(11): 961–968, doi: [10.1097/MNM.0000000000000889](https://doi.org/10.1097/MNM.0000000000000889), indexed in Pubmed: [30106798](https://pubmed.ncbi.nlm.nih.gov/30106798/).
9. Gross AM, Wolters PL, Dombi E, et al. Selumetinib in children with inoperable plexiform neurofibromas. *N Engl J Med.* 2020; 382(15): 1430–1442, doi: [10.1056/NEJMoa1912735](https://doi.org/10.1056/NEJMoa1912735), indexed in Pubmed: [32187457](https://pubmed.ncbi.nlm.nih.gov/32187457/).